

Analyst

Accepted Manuscript



This is an *Accepted Manuscript*, which has been through the Royal Society of Chemistry peer review process and has been accepted for publication.

Accepted Manuscripts are published online shortly after acceptance, before technical editing, formatting and proof reading. Using this free service, authors can make their results available to the community, in citable form, before we publish the edited article. We will replace this *Accepted Manuscript* with the edited and formatted *Advance Article* as soon as it is available.

You can find more information about *Accepted Manuscripts* in the [Information for Authors](#).

Please note that technical editing may introduce minor changes to the text and/or graphics, which may alter content. The journal's standard [Terms & Conditions](#) and the [Ethical guidelines](#) still apply. In no event shall the Royal Society of Chemistry be held responsible for any errors or omissions in this *Accepted Manuscript* or any consequences arising from the use of any information it contains.

1
2
3
4
5
6
7
8
9
10
11
12
13
14
15
16
17
18
19
20
21
22
23
24
25
26
27
28
29
30
31
32
33
34
35
36
37
38
39
40
41
42
43
44
45
46
47
48
49
50
51
52
53
54
55
56
57
58
59
60

2,4-Toluene Diisocyanate Detection in Liquid and Gas Environments Through Electrochemical Oxidation in an Ionic Liquid

Lu Lin, Abdul Rehman, Xiaowei Chi, Xiangqun Zeng*

Department of Chemistry, Oakland University, Rochester, MI 48309, USA

* Corresponding Author (Email: zeng@oakland.edu)

ABSTRACT

The electrochemical oxidation of 2,4-toluene diisocyanate (2,4-TDI) in an ionic liquid (IL) has been systematically characterized in order to determine the plausible electrochemical and chemical reaction mechanism and to define the optimal detection methods for such a highly significant analyte. It has been found that the use of an IL as the electrolyte allows the oxidation of 2,4-TDI to occur at less positive anodic potential with no side reactions as compared to traditional acetonitrile based electrolytes. UV-Vis, FT-IR, Cyclic Voltammetry and Electrochemical Impedance Spectroscopy (EIS) studies have revealed the unique mechanisms of dimerization of 2,4-TDI at the electrode interface by self-addition reactions which can be utilized to improve the selectivity of detection. The study of 2,4-TDI redox chemistry further facilitates the development of a robust amperometric sensing methodology by selecting a hydrophobic IL ([C₄mpy][NTf₂]) and by restricting the potential window to only include the oxidation process. Thus, this innovative electrochemical sensor has been made capable to avoid the two most ubiquitous interferents of the ambient conditions (i.e. humidity and oxygen) thereby enhancing the sensor performance and reliability for real world applications. The method was established to detect 2,4-TDI in both liquid and gas phases. The limits of detection (LOD) values are 130.2 ppm and 0.7862 ppm, respectively for the two phases, and are comparable to the safety standards reported by NIOSH. The so developed 2,4-TDI amperometric sensor exhibits a sensitivity of 1.939 μ A/ppm. Moreover, due to the simplicity of design and the use of an IL both as a solvent and non-volatile electrolyte, the sensor has the potential to be miniaturized for smart sensing protocols for the distributed sensor applications.

INTRODUCTION

Recent explosions in Tianjin, the port city of China where chemicals such as toluene diisocyanates (2,4-TDI) and calcium carbide has been stored thereby killing more than 50 people leaving several hundred injured, has reemphasized the need of detection of these compounds in liquid and gas phase with minimum human intervention.¹ As reported, diisocyanates² are low molecular weight, and significantly toxic compounds violently reacting with water and other chemicals causing explosions, yet highly valuable in manufacturing industry of polyurethane-based products, such as foams, elastomers and coatings. These products are everywhere in people's daily life because of their durability against chemical damages, color stability, and abrasive resistance. However, their manufacturing processes and the product degradation causes the diisocyanates to be airborne thereby posing an adverse challenge for environmental protection and occupational health.^{3,4} Additionally, their short-term exposure can cause allergic sensitization, severe irritation of the skin and eyes as well as problems in respiratory, gastrointestinal and even the central nervous systems whereas the long-term exposure can affect the lung function.⁵ Results from animal studies have also reported a significant increase of tumor cells in organs such as pancreas, liver and mammary glands after exposure to diisocyanates.⁶ Therefore, diisocyanates have been classified as Group 2B (possible human carcinogen) by the International Agency for Research on Cancer (IARC).

In order to avoid these adverse health, environmental, and even life safety threats, accurate and fast diisocyanates detection in real world environments is extremely significant. Both instrumental and continuous monitoring methods have been developed in this regard as reviewed by Guglya.² As shown in Table S1, for the instrumental methods,⁷ such as high performance liquid chromatography (HPLC),^{8,9} capillary gas chromatography (CGC) with flame

1
2
3 ionization^{10, 11} and ion chromatography with UV detection,^{12, 13} the derivatization and extraction
4
5 steps are quite time-consuming. Moreover, such offline strategies provide significant statistical
6
7 differences as compared to online protocols.¹⁴ On the other hand, the most conventional
8
9 colorimetric method¹⁵ has interference problems especially from humidity in the air. Infrared
10
11 spectrophotometric method¹⁶ based on quantitative measurements of C-H deformation vibration
12
13 at the aromatic ring has also been reported, however, it requires large sampling amount and
14
15 multiple steps of sample preparation. Biological monitoring including the measurement of
16
17 diisocyanate specific antibodies in serum, diisocyanate derived biomarkers in blood and urine, or
18
19 the ELISA based methods have also been studied,¹⁷ but these methods lack the specificity for
20
21 different diisocyanates while specialized instrumentation is a requirement. Smart sensors can be
22
23 an efficient substitution in such a situation which can continuously monitor these hazardous
24
25 compounds in actual workplace conditions. Morrison et al made the first attempt in this regard
26
27 using coated piezoelectric crystals.¹⁸ However, the universal sensitivity of the technique make it
28
29 unsuitable for measurement especially in humid environments. Electrochemical sensors are
30
31 historically proven to be an ideal detection platform due to its simplicity in design, direct
32
33 transduction signal readout, fast response time, good selectivity and sensitivity.^{19-21, 22, 23}
34
35 Electrochemical sensors require the use of an electrolyte, diisocyanates are not stable in many
36
37 conventional electrolytes especially aqueous electrolytes limiting the development of such
38
39 electrochemical sensors.
40
41
42
43
44
45
46
47

48
49 Ionic liquids (ILs) on the contrary has such unique features²⁴ that resist to chemical
50
51 interferences and facilitate new electrochemical reactions to occur which otherwise are not
52
53 feasible in traditional aqueous or non-aqueous electrolytes. The benefits of ILs for
54
55 electrochemistry has been summarized in Liu et al²⁵ research review of interface chemistry of
56
57
58
59
60

1
2
3 IL/electrode. Our group has been utilizing the benefits of ILs in developing gas sensors over past
4
5 ten years.²⁶⁻³¹ In many of gas sensor applications, the presence of oxygen being ubiquitous in
6
7 nature, interfere strongly with electrochemical processes by forming superoxide radical and thus
8
9 complicating the sensor performance. The superoxide radical has been reported to be relatively
10
11 stable in ILs and is positively utilized for mechanism explorations and sensing
12
13 enhancements.^{27,32,33} However, such reactions if can be avoided could simplify the sensor
14
15 developments. In the current work, we developed a simple electrochemical method for direct,
16
17 qualitative and quantitative isocyanates detection, with the capability for future sensor
18
19 miniaturization. As one of the most common airborne isocyanates, 2,4-TDI was selected as the
20
21 representative analyte for this study. Isocyanates react with water, alcohols, acids, and organic
22
23 solvents that have primary or secondary amine functional group.³⁴ The extent of their reactivity
24
25 depends on the activity of hydrogen species in the solvent compounds, the steric hindrance,
26
27 basicity and the electronegativity of the substituent side groups of the solvent molecules.
28
29 Therefore, non-aqueous solvent systems without primary or secondary amine, but with lower
30
31 basicity and larger electronegativity branch chains are preferred for isocyanate detection. Based
32
33 on this, an ionic liquid [C₄mpy][NTf₂] was chosen as the solvent as well as the supporting
34
35 electrolyte because the pyrrolidinium cation is relatively chemically inert and all C-H bonds in
36
37 the [C₄mpy]⁺ cation structure are saturated. Moreover, [NTf₂]⁻ based ILs with conjugated
38
39 structures exhibit better electrochemical stability than others such as [BF₄]⁻ and [PF₆]⁻ based
40
41 ones.²⁷ We first investigated the redox processes of 2,4-TDI in ILs as well as its redox
42
43 mechanism at the electrochemical interface. Based on the knowledge gained in the mechanistic
44
45 study, we developed a new electrochemical methodology for detection of 2,4-TDI in liquid phase
46
47 as well as gas phase. The analytical performance of the so presented electrochemical ionic liquid
48
49
50
51
52
53
54
55
56
57
58
59
60

1
2
3 sensor meets the safety standards of National agencies, and thus the sensor is envisioned to be
4
5 competitive compared to the commercial available technologies for diisocyanates detection.
6
7

8 9 **EXPERIMENTAL SECTION**

10
11 **Chemicals.** 2,4-toluene diisocyanate (2,4-TDI) (**Scheme S1A**) was purchased from *Fluka* with
12
13 99.9% purity. 1-butyl-1-methylpyrrolidinium bis(trifluoromethylsulfonyl) imide which was
14
15 abbreviated as [C₄mpy][NTf₂] or [Bmpy][NTf₂] (**Scheme S1B**) was purchased from *Ionic*
16
17 *Liquids Technologies Inc.* with 99% purity and was stored in a vacuum dry chamber (*Shel Lab*
18
19 model no. 1415M) under room temperature and a vacuum pressure up to 18 inch Hg.
20
21 Tetrabutylammonium perchlorate (TBAP) was purchased from *Fluka* with assay grade (\geq
22
23 99.0%). Prior to the measurements, IL aliquots were purged with N₂ (*Airgas* compressed
24
25 nitrogen) for 12 hours in order to exclude the O₂ and moisture as well as to maintain the same
26
27 electrolyte condition. Dry air (*Airgas*, breathing grade) was utilized as the background gas for
28
29 most characterization tests.
30
31
32
33
34
35

36
37 **Electrodes.** Planar glassy carbon electrode (purchased from *CH Instruments, Inc.*) was used as
38
39 the working electrode. The geometric surface area was 0.0707 cm². The reference and counter
40
41 electrodes were silver wire and platinum wire, respectively. The diameters for both these
42
43 electrodes were 0.5 mm. The working electrode was first polished using *Buehler* micropolish 1.0
44
45 micron alpha alumina-water slurry followed by 0.05 micron gamma alumina-water slurry, then
46
47 sonicated using *Branson* 3510 ultrasonic unit with deionized water for 10 minutes. In the final
48
49 step, the electrode was rinsed with deionized water and dried with N₂ immediately. In order to
50
51 eliminate the influence from the potential drift of the silver quasi reference electrode, we used
52
53 Fc/Fc⁺ redox couple to calibrate the potentials. For gas phase detection, the carbon electrode was
54
55
56
57
58
59
60

1
2
3 prepared by loading a graphite ink onto a Teflon membrane (*Interstate*, PM71W). The ink³⁶
4 consists of 40.62 mg graphite (*Aldrich*, < 20 μm , synthetic), 768 μL water, 200 μL ethanol and
5
6
7
8 32 μL 5 wt.% Nafion water dispersion (*Aldrich*). The loading amount is 10.35 mg/cm^2 .
9

10
11 **Electrochemical Cell.** A conventional three electrode cell was employed in this work. The
12 electrodes were fixed via Teflon tape and housed in a glass tube, a cross section of which is
13
14 shown in **Scheme S1C**. The bottom part of this cell was immersed in silica oil bath set at room
15
16 temperature (25 $^{\circ}\text{C}$). Pure N_2 flew into the electrochemical cell via *Tygon* PVC gas tubing ($\phi = 1$
17
18 mm). The gas was then left to diffuse through the IL until the gas pressure reached an
19
20 equilibration state between the gas and liquid phases prior to the measurements. This typically
21
22 takes about 30 minutes. The gas outlet was connected to the vacuum vent to avoid buildup of gas
23
24 in the electrochemical cell.
25
26
27
28
29

30 31 **Electrochemical Experiments**

32
33
34 The *Gamry* 4-channel workstation was used to perform CV, EIS and
35
36 Chronoamperometry measurements of 2,4-TDI redox processes. For EIS measurements, a 5 mV
37
38 AC voltage was applied under open circuit condition. Initial experiments involved adding 2,4-
39
40 TDI to the ionic liquid, mixed, and degassed by N_2 before each measurement.
41
42 Chronoamperometry measurements were performed for detection of gas phase 2,4-TDI. Since
43
44 2,4-TDI has a vapor pressure of 0.05 mmHg at 25 $^{\circ}\text{C}$,³⁵ the gas phase 2,4-TDI was generated by
45
46 bubbling air through 2,4-TDI liquid. It was subsequently diluted with another air gas flow via
47
48 two *Tygon* PVC gas tubings ($\phi = 1$ mm), one of which was the pure air gas channel (path 1) and
49
50 the other was the channel (path 2) to bring out the gas phase 2,4-TDI by air flow. A cross-section
51
52 of this sampling system is depicted in **Scheme S2**. Total gas flow rate was maintained at 200
53
54
55
56
57
58
59
60

1
2
3
4
5
6
7
8
9
10
11
12
13
14
15
16
17
18
19
20
21
22
23
24
25
26
27
28
29
30
31
32
33
34
35
36
37
38
39
40
41
42
43
44
45
46
47
48
49
50
51
52
53
54
55
56
57
58
59
60

sccm. Concentrations of gas phase 2,4-TDI were prepared by increasing the flowrate of path 2 from 0 to 100 sccm, with 20 sccm per increment. Such a gas sensor testing system has been described in detail elsewhere.³⁶ The detail calculation of TDI concentration in this flow system is elaborated in the supplementary information.

RESULTS AND DISCUSSION

Characterization of 2,4-TDI Redox Processes

Effects of the Supporting Electrolyte and Environmental Conditions

Ionic liquids (ILs) have been shown to have a significant effect on the redox behavior of organic compounds. These effects can be the shifting of oxidation and/or reduction potentials, stabilizing the redox reaction products inducing certain additional chemical reactions, or even the changes of electrochemical reaction mechanisms (e.g., the two one-electron reduction waves of dinitrobenzene in acetonitrile is reportedly collapsed to a single two-electron wave in ILs such as [C₄mim][BF₄]).³⁷ Such anomalies due to the presence of IL electrolytes are usually ascribed to strong ion-pairing in ILs. In a series of computational studies, Fry et al³⁸ has examined and reported the interactions between solvent, electrolytic ions, and electroactive species indicating the redox potentials can be lowered when the ion-pairing with the electrolyte was included. We hypothesize that the similar shifts in the oxidation mechanisms of analytes (i.e., 2,4-TDI) can have significant implications on the development of a more efficient isocyanate electrochemical sensor. Therefore cyclic voltammetry (CV) was first utilized to characterize an isocyanate redox activity in two non-aqueous solvents (i.e., acetonitrile and IL [C₄mpy][NTf₂]). **Figure 1A** presents the cyclic voltammogram of 2,4-TDI in both solvents whereas nitrogen was used as the

1
2
3 background. In the case of acetonitrile, the oxidation of 2,4-TDI occurred at 1.96 V. On the other
4
5 hand, there was no redox peak observed in the pure IL indicating that electrochemical system
6
7 comprising IL is stable in this potential region. In the presence of 2,4-TDI in the IL,
8
9 electrochemical oxidation peak of 2,4-TDI was observed at a less positive anodic potential (1.38
10
11 V) than it was in acetonitrile (1.96 V). Moreover, though the oxidation peak currents have
12
13 similar values in both electrolytes, multiple shoulder peaks and a broad small reduction peak
14
15 were observed before the major oxidation peak in acetonitrile system, suggesting that 2,4-TDI
16
17 oxidation process in acetonitrile involves multiple steps. Such complicated redox mechanisms
18
19 usually cause difficulty in quantitative analysis due to poor reproducibility and are not desirable
20
21 for electroanalytical method development. Contrarily, in [C₄mpy][NTf₂] system, it showed single
22
23 and clear oxidation peak which can be used for analytical quantification. Thus, utilization of
24
25 [C₄mpy][NTf₂] was validated to be suitable for electrochemical detection of 2,4-TDI as has been
26
27 done in our group for various different analyte targets.^{28, 30, 31, 33, 39} In [C₄mpy][NTf₂], the
28
29 oxidation peak current of 2,4-TDI was approximately seven times larger than that of the
30
31 reduction peak, as shown in (**Figure 1A**). Therefore, it is also clear that the oxidation process is
32
33 capable to provide better sensitivity for the detection of 2,4-TDI (**Figure 1B**) and can be used for
34
35 further quantifications. It was also found that the reduction process would interfere the current
36
37 signals of the oxidation process as well. As shown in **Figure 1A**, when the reduction process
38
39 occurred first, the 2,4-TDI concentration would decrease in the region near the electrode surface
40
41 leading to a decreased TDI oxidation signal as compared to the narrower potential scan in
42
43 **Figure 1B** (i.e. the oxidation peak current in **Figure 1B** was 381 μ A, higher than the value of
44
45 297 μ A in **Figure 1A**). Thus, in real sensing development, the potential region is selected where
46
47
48
49
50
51
52
53
54
55
56
57
58
59
60

only oxidation of 2,4-TDI occurs. Above experiments supported us to study the optimal 2,4-TDI sensing conditions as well as demonstrate the benefit to employ IL in these sensor developments.

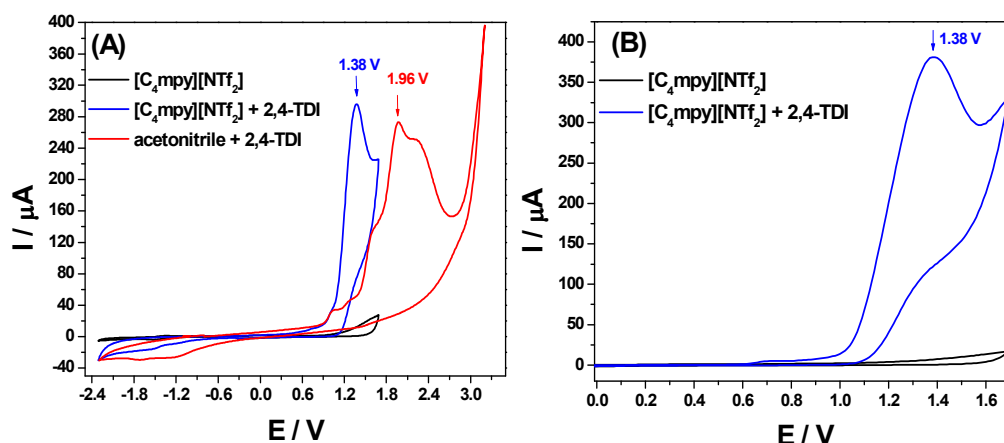
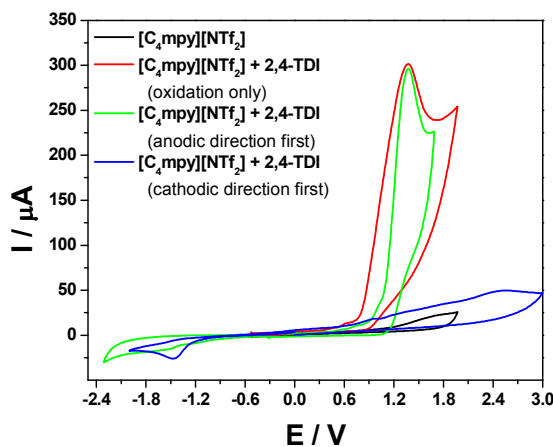


Figure 1. (A) CV of pure $[C_4mpy][NTf_2]$ (black), 1% v/v 2,4-TDI $[C_4mpy][NTf_2]$ (blue), and 1% v/v 2,4-TDI in acetonitrile with 0.1 M TBAP as supporting electrolyte (red). The concentration was 1.0% v/v. Glassy carbon, silver and platinum electrodes were used as the working, reference and counter electrodes, respectively. Scan rate was 100 mV/s. All potentials were calibrated based on the Fc/Fc^+ redox couple. N_2 was used as background gas. CV scanned toward the negative potential direction first. (B) CV for 1 mL pure $[C_4mpy][NTf_2]$, and in the presence of 1% v/v 2,4-TDI in the potential window of 0 to 1.7 V. All curves presented here are taken from the first cycle of the CV measurements.

In order to further investigate the electrochemical process of 2,4-TDI and to mimic the real world sensing conditions, similar cyclic voltammetric experiments were conducted using air as the background gas as shown in **Figure 2**. Oxygen is ubiquitous in the ambient environment playing significant roles in any sensing method development. Especially, its presence can also modify the electrochemical processes in ILs, even though the reductively generated superoxide anion radical is more stable than in other solvents. Xiao et al has reported the effect of the superoxide radical on the carbon dioxide electrochemistry.³³ Herein, it is shown that for a narrow potential scan where oxygen reduction process is not involved, a clear and large 2,4-TDI oxidation peak was observed (red curve). Same was true for the experiment for a wider potential window, but with initiating the scan in the anodic direction thereby performing the 2,4-TDI oxidation before its reduction (green curve). However, when the scan direction was first in the

1
2
3 cathodic potential, involving the generation of superoxide shown by a reduction peak at ~ -1.4 V,
4
5 the peak for the oxidation of 2,4-TDI was almost disappeared (see the blue curve). From this data,
6
7 two important conclusions can be drawn. First, 2,4-TDI can react with the reduction products of
8
9 most important environmental interferent, oxygen,⁴⁰ thereby leaving no TDI at the interface to be
10
11 detected. This property can be used for removing toxic TDI but supporting the choice of using
12
13 only the oxidation processes for quantification as shown by the results of these experiments,
14
15 especially if the electrochemical 2,4-TDI sensor has to be used in real ambient environments.
16
17 Second, this experiment also shows the selectivity of the sensing system for 2,4-TDI under the
18
19 chosen experimental conditions. The peak at 1.38 V is clearly due to the presence of 2,4-TDI,
20
21 which remains there in the presence of oxygen and all other air gases, although it disappears in
22
23 the presence of superoxide due to their reaction. Thus, if the formation of superoxide radical is
24
25 avoided by choosing a specific potential window, 2,4-TDI can be selectively detected in real
26
27 ambient environments.
28
29
30
31
32
33
34
35



51 **Figure 2.** CV of pure $[C_4mpy][NTf_2]$ (black), in the presence of 1.0% v/v 2,4-TDI in the narrow
52 anodic potential window (red), in wider potential window scanning to the anodic potential direction
53 first (green), and in wider potential window scanning to the cathodic potential direction first to
54 form superoxide radical thereby showing no oxidation current for 2,4-TDI (blue). Air was the
55 background gas for all these measurements. All curves presented here are taken from the first cycle
56 of the CV measurements.
57

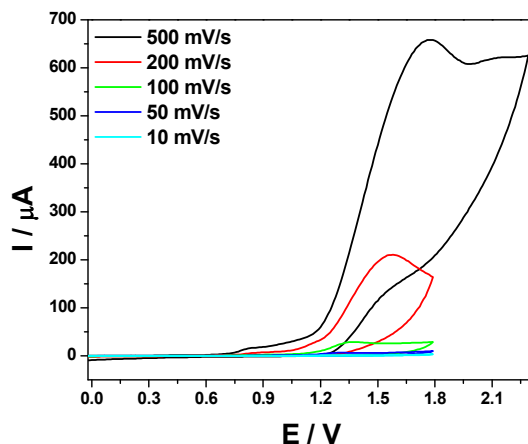


Figure 3. CV of 0.1% v/v 2,4-TDI in [C₄mpy][NTf₂] with the variation of scan rates. Glassy carbon, silver and platinum electrodes were used as the working, reference and counter electrodes, respectively. All potentials were calibrated based on Fc/Fc⁺ redox couple. Air was the background gas for all these measurements. All curves presented here are taken from the first cycle of the CV measurements.

For further elaboration of the electrochemical reaction mechanisms for the above processes, we performed the CV at various scan rates. **Figure 3** shows the cyclic voltammogram of 0.1% v/v 2,4-TDI in [C₄mpy][NTf₂] at scan rates of 10 mV/s – 500 mV/s. An oxidation peak potential shift (from 1.77 V to 1.24 V) was observed when the scan rate was changed from 500 mV/s to 10 mV/s. For a fast electrochemically reversible system, the peak potential does not shift at different scan rates. In 2,4-TDI case, the electrode reaction is an irreversible process even at a slow scan rate (e.g. 10 mV/s). Thus, the peak potential shift is suggested to be the results of multiple coupled reactions, e.g. chemical reactions coupled with the electrochemical reactions or the electron transfer reaction reactions rather than the uncompensated IR drop, based on the following results: 1) the peak current has linear relationship with the scan rate supporting a surface controlled electron transfer process; 2) the increase of impedance vs. frequency in EIS measurement at various time intervals (**Figure 5**) supporting the surface reactions discussed below.

1
2
3
4
5
6
7
8
9
10
11
12
13
14
15
16
17
18
19
20
21
22
23
24
25
26
27
28
29
30
31
32
33
34
35
36
37
38
39
40
41
42
43
44
45
46
47
48
49
50
51
52
53
54
55
56
57
58
59
60

Furthermore, it is important to note in **Figure 3** that a shoulder peak started to emerge at about 0.8 V. This is more evident at faster scan rates. Kuroiwa et al⁴¹ has reported a similar shoulder peak for the oxidation reaction of chlorophyll a in IL/acetonitrile mixture, whereas this peak can be de-convoluted from the voltammogram and the resulting peak current can be estimated by using Gaussian curve fitting method. The peak current ratio of P_I/P_{II} decreases as the scan rate increases (from 0.251 at 10 mV/s to 0.0254 at 500 mV/s) where P_I is the shoulder peak and P_{II} is the main oxidation peak, which suggests that the first oxidation process (P_I) has a relatively slower kinetics and can be related to the aggregation of the analyte molecules as was the case with chlorophyll a. Furthermore, the sufficiently large oxidation current for this peak strongly supports the idea that analyte molecules form quite a low-order aggregate such as a dimer, since high-order aggregates would not yield sizeable oxidation current due to slow diffusion. Such aggregation process has been reported to lower the oxidation potential of the analyte in addition to similar effects caused by IL ion-pairing. To further investigate this peak P_I and to validate the possibility of dimerization process, a series of CV measurement with different time intervals were designed. In this experiment, 2,4-TDI was equilibrated in the IL electrolytes at different times and then the measurements are performed. The 2,4-TDI oxidation peak current decreased when the CV measurements were performed at longer time intervals (**Figure 4**). No peak potential shift was observed as was the case during the variation of scan rates. The peak current values followed a first-order exponential decrease (**Figure 4B**) with a correlation coefficient equal to 0.994. This exponential decay of the 2,4-TDI oxidation peak current can also be utilized for the selectivity study of the future sensor device. In **Figure 4**, the shoulder oxidation peak (P_I , located at 0.8 V) was also observed. This peak was more obvious at longer time intervals (e.g., 1000 min) and fairly insignificant when the measurement was carried out

instantly (0 min). The reduced current signals for P_{II} and increasing current signals for P_I with increasing time of measurement could only be attributed to the adsorption of 2,4-TDI at electrode surface by the formation of dimers, trimers and even polymers through isocyanate self-addition reactions (eq.1 & eq.2 where R is defined as the toluene aromatic ring), which lowered the concentration of electrochemically active species near the electrode surface.

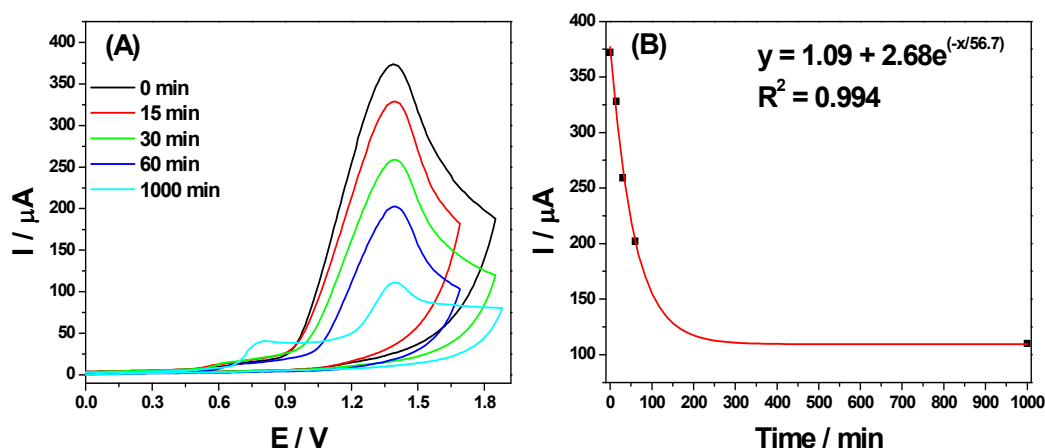
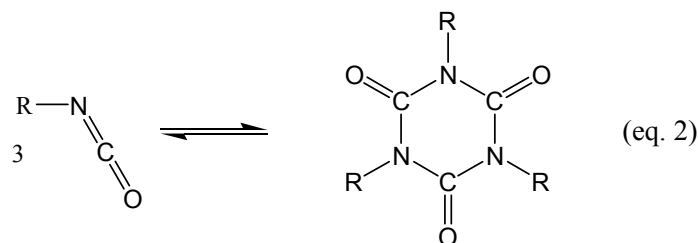
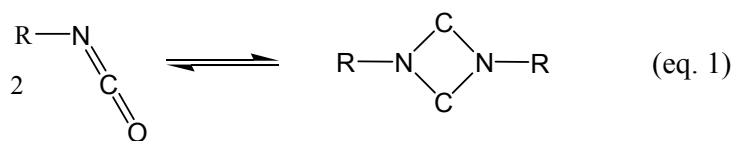


Figure 4. (A) CV of 2,4-TDI oxidation process in $[C_4mpy][NTf_2]$ in the air environment, on glassy carbon electrode. The concentration of 2,4-TDI was 10 μ L in 1 mL ionic liquid (1.0% v/v). Silver and platinum wires were the reference and counter electrodes, respectively. Measurements were performed with different time intervals after the three-electrode system had been setup. Scan rate was 100 mV/s. All potentials were calibrated based on Fc/Fc^+ redox couple. All curves presented here are taken from the first cycle of the CV measurements. (B) The corresponding calibration curve. Air was the background gas for all these measurements.



1
2
3 We performed electrochemical impedance analysis to understand further about the
4 interface reactions at different time scales. EIS results can provide valuable information about
5 the dynamic surface adsorption processes of 2,4-TDI in the [C₄mpy][NTf₂] electrolyte. EIS has
6 been used to study many surface reactions such as the dyes and surfactants dimerization
7 processes.⁴² Thus, EIS experiments were carried out at several time intervals in the presence of
8 2,4-TDI at open circuit potential. As shown in **Figure 5A** and **Figure S3**, the Nyquist plots
9 changes at various time of the measurements. As shown in **Figure S3**, We simulated the EIS
10 curves by carefully selecting the equivalent circuit, according to the literature. Among all the
11 equivalent circuit models we employ to fit the experimental data, the one that gives the best fit is
12 presented in the inset of **Figure S3**. These simulated results are not good fit especially at zero
13 hours. We believe that the deviation from the perfect fit is an indication for the dynamic
14 chemical reactions (i.e. the TDI self-polymerizations). **Figure 5B**, the Bode curves of the EIS
15 experiment presents correlation of $\log|Z|$ versus \log frequency at different time intervals. The Z'
16 versus frequency and Z'' versus frequency plots (**Figure S3 C-D**) show that the real part of the
17 impedance increases with time at low frequencies much more than the imaginary part of the
18 impedance. It is obvious that the surface reactions cause the impedance to increase at longer time
19 intervals especially at low frequencies. Such trend can also be observed in the Nyquist plots too
20 (**Figure 5A**) and are similar to the ones reported earlier for different surfactants and dyes in
21 dimerization/aggregation reactions.
22
23
24
25
26
27
28
29
30
31
32
33
34
35
36
37
38
39
40
41
42
43
44
45
46
47
48

49 Results from the EIS experiment confirm the dynamic interface processes of 2,4-TDI and
50 are consistent with the results presented in **Figure 4**. Toluene was used as a negative control to
51 further understand the 2,4-TDI oxidation processes in the IL at glassy carbon electrode. The
52 selection of toluene as reference sample was due to its similar chemical structure as 2,4-TDI
53
54
55
56
57
58
59
60

except the two isocyanate groups ($-N=C=O$). No oxidation peak was observed in toluene sample with the same conditions as for 2,4-TDI. Thus, the oxidation peak and the consequent surface modification/dimerization are attributed to the isocyanate groups.

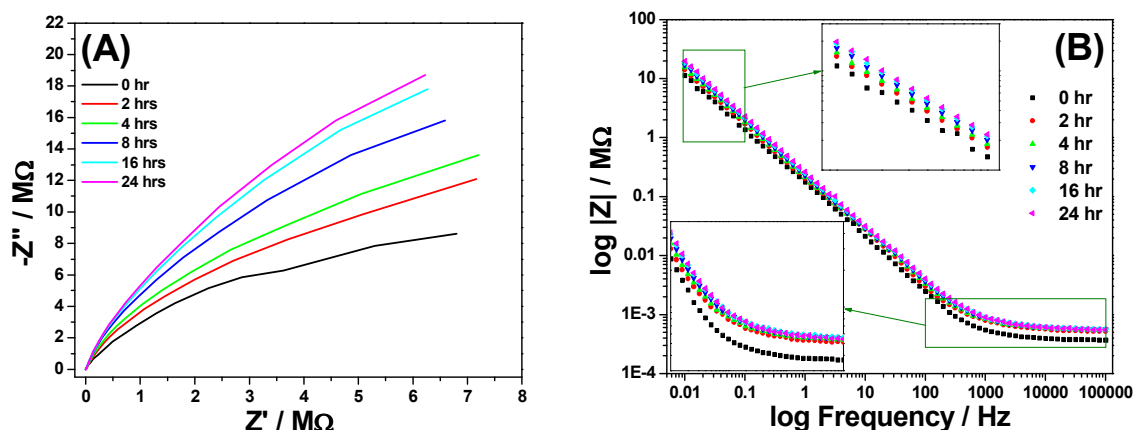


Figure 5. (A) Nyquist plots measured at various time intervals with 1% v/v 2,4-TDI in $[C_4mpy][NTf_2]$ on glassy carbon electrode. Silver wire and platinum wire were the reference and counter electrodes, respectively. (B) The Bode plots measured at various time intervals with 1% v/v 2,4-TDI in $[C_4mpy][NTf_2]$ on glassy carbon electrode. Silver wire and platinum wire were the reference and counter electrodes, respectively. (C) The Bode plots of Z' (the real part of the impedance) changes at different frequencies. (D) The Bode plots of Z'' (the imaginary part of the impedance) changes at different frequencies. The EIS experimental parameters: AC bias was 5 mV, and the DC input was 0 V vs. open circuit. Air is the background gas.

Identifications of Interface Products by UV-vis and FT-IR

UV-vis and FT-IR spectroscopy experiments were employed to determine the 2,4-TDI oxidation products to allow additional insights on the reaction mechanism. There are two possible molecular sites for 2,4-TDI oxidation: 1) the C-N single bond cleavage at the 2 and/or 4 position of the benzene ring, or 2) the N=C double bond cleavage in the isocyanate functional group. First, UV/vis measurements (**Figure 6A**) were performed to characterize samples of different 2,4-TDI concentrations in $[C_4mpy][NTf_2]$ as well as the sample of pure $[C_4mpy][NTf_2]$

as the background. As the concentration of 2,4-TDI increased, the absorbance peak at 290~300 nm⁴³ also increased with a red shift, indicating an enhanced delocalized conjugation effect. This could be attributed to the isocyanates self-additions forming isocyanate polymers. We also characterized the bulk IL near the glassy carbon electrode surface after an electrochemical oxidation of 2,4-TDI was conducted. A significant decrease of the absorbance and a blue shift were observed from this bulk IL sample. The absorbance peak changes indicated that there was a reduced conjugation of the 2,4-TDI molecular structure, which could be attributed to the loss of isocyanate functional group due to electrochemical oxidation of 2,4-TDI, causing a decrease of the delocalized conjugation effect.

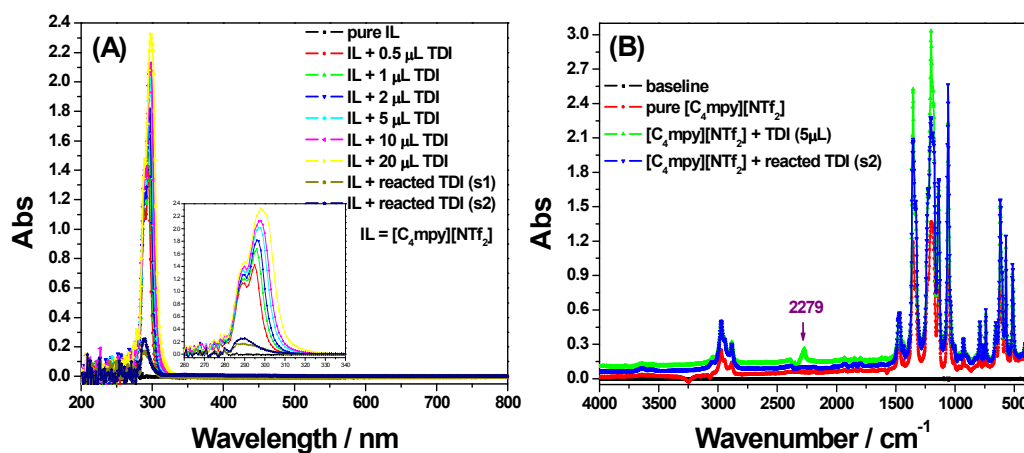
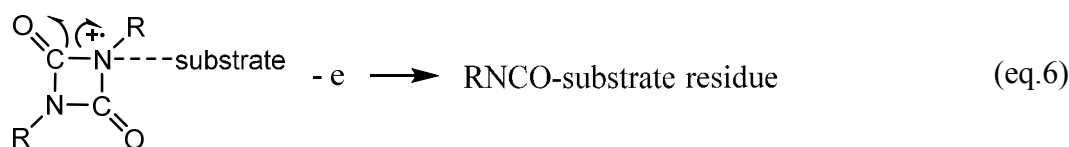
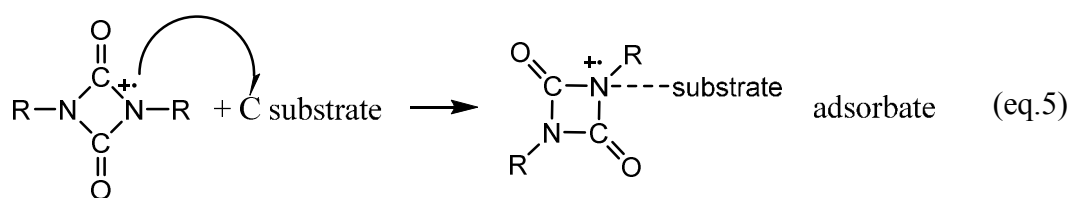
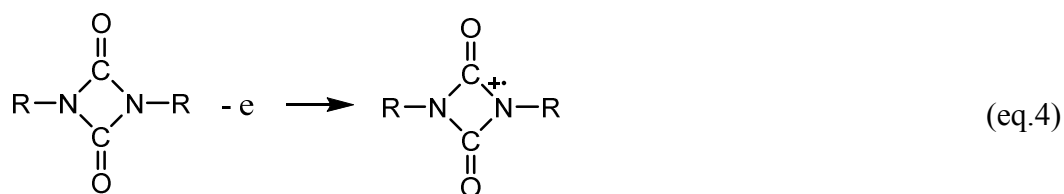


Figure 6. Spectroscopic characterization of the electrochemical reaction of 2,4-TDI in [C₄mpy][NTf₂] on glassy carbon surface: (A) UV/vis method, and (B) FTIR method (transmission mode). 2,4-TDI concentration varied from 0.05% v/v to 2% v/v.

FT-IR measurements (**Figure 6B**) were carried out to obtain additional information in terms of identifying the bond breaking of the isocyanate functional group. An absorbance peak at 2279 cm⁻¹ was observed from [C₄mpy][NTf₂] in the presence of 0.5% v/v 2,4-TDI. This peak was not found in either pure [C₄mpy][NTf₂] or [C₄mpy][NTf₂] sample that was taken from the

1
2
3 bulk solution near the glassy carbon electrode surface after an electrochemical oxidation of 2,4-
4 TDI was previously performed. According to Thomson et al.,⁴⁴ absorbance peak at 2279 cm⁻¹
5 could be assigned to the asymmetric vibration of N=C=O functional group. This illustrated that
6 the NCO functional group disappeared. Thus, it is plausible that the N=C double bond was
7
8
9
10
11
12
13
14
15
16
17
18
19
20
21
22
23
24
25
26
27
28
29
30
31
32
33
34
35
36
37
38
39
40
41
42
43
44
45
46
47
48
49
50
51
52
53
54
55
56
57
58
59
60

bulk solution near the glassy carbon electrode surface after an electrochemical oxidation of 2,4-TDI was previously performed. According to Thomson et al.,⁴⁴ absorbance peak at 2279 cm⁻¹ could be assigned to the asymmetric vibration of N=C=O functional group. This illustrated that the NCO functional group disappeared. Thus, it is plausible that the N=C double bond was cleaved during 2,4-TDI oxidation. Thus, the plausible mechanism is then an CECE mechanism depicted as follows (R is defined as the toluene aromatic ring, we use the dimer as a case study), in which the chemical process is the rate limiting step:



1
2
3 2,4-TDI monomer undergoes a self-addition reaction in the initial state (eq. 3). When an external
4
5 anodic potential is applied, eq. 4 occurs yielding a stable radical product due to the delocalized
6
7 electron conjugation effect. It is followed by a surface adsorption process (eq. 5, C stands for
8
9 glassy carbon) at anodic condition. This step is the rate limiting one because of the reactivity of
10
11 carbon surface. Then, a second oxidation occurs involving the C-N bond breaking forming
12
13 adsorbate residues (eq. 6). This proposed mechanism complies with CV data in **Figure 4** that the
14
15 shoulder peak becomes more significant at longer testing time intervals.
16
17
18
19
20
21
22

23 **Sensing Characterization of TDI Oxidation in ILs**

24
25
26 Once the mechanisms of the electrochemical oxidation of 2,4-TDI has been understood
27
28 using electrochemical, EIS, and spectroscopic techniques, we now had the guidelines to design
29
30 electrochemical methods for evaluating the sensing performance utilizing the resulting
31
32 mechanism. Usually, the sensor is first employed to do sensitivity tests by exposing it to different
33
34 concentrations of the analyte. However, we first performed the selectivity tests in order to clear
35
36 out following important points of the study. First, the selectivity experiments for the compounds
37
38 similar to the molecule under study can provide an indirect proof of dimerization process
39
40 suggested for 2,4-TDI. Second, the presence of dimerization if it is the case with only the TDI,
41
42 the detection/sensing mechanism can be made very selective which is most important
43
44 requirement of present day sensors.
45
46
47
48
49

50 Selectivity experiments for 2,4-TDI

51
52
53 2,4-TDI was selected as the representative molecule of the isocyanates, since it has high
54
55 vapor pressure of 0.05 mm Hg and is the most common airborne. As described earlier, toluene
56
57
58
59
60

1
2
3
4
5
6
7
8
9
10
11
12
13
14
15
16
17
18
19
20
21
22
23
24
25
26
27
28
29
30
31
32
33
34
35
36
37
38
39
40
41
42
43
44
45
46
47
48
49
50
51
52
53
54
55
56
57
58
59
60

can be used as negative control for 2,4-TDI oxidation process as it has the same structure with the absence of isocyanate groups. However, it can also be tested as interfering molecule for 2,4-TDI detection. When toluene was subjected to the electrochemical oxidation process, no oxidation peaks were observed as shown in **Figure S1** even for a concentration of 4%. In the same experiment, TDI at much lower concentration showed reproducible signals. In the other experiment, aniline which is quite well known oxidizable compound is tested in comparison to 2,4-TDI. At the same concentration and under the same conditions, aniline showed an oxidation current even larger than the target (**Figure S2**), though the peak potential of aniline is quite different. Thus, different electrochemical techniques such as chronoamperometry can be used to selectively detect the target isocyanates by choosing a certain measurement potential.

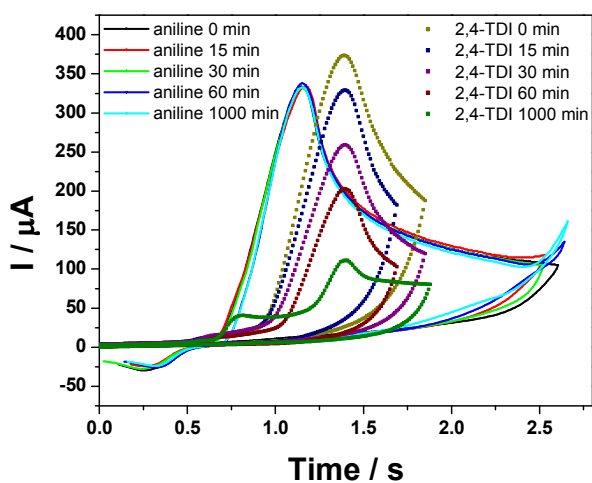


Figure 7. CV of $[C_4mpy][NTf_2]$ adding 1% v/v aniline (straight lines) and 1% v/v 2,4-TDI (dotted lines), at different testing time intervals, at air condition. Glassy carbon, silver and platinum electrodes were used as the working, reference and counter electrodes, respectively. Measurements were performed with different time intervals after the three-electrode system had been setup. Scan rate was 100 mV/s. All potentials were calibrated based on Fc/Fc^+ redox couple. All curves presented here are taken from the first cycle of the CV measurements.

However, the most important observation in this regard came from the time lapse experiment done with aniline and 2,4-TDI, the data is shown in **Figure 7**. As indicated, no

significant change in the oxidation current signal occurs in the IL that contains aniline but the same shoulder peak is present in IL containing TDI thereby decreasing the oxidation peak current with every time step. This indirectly proves the self-addition reaction of TDI, and alongside, this mechanism can serve to provide extremely selective response mechanism of TDI detection with signal diminishing as a function of time. Additionally, Yakabe et al⁴⁵ reported that aniline and 2,4-TDI exhibit different side reactions in the presence of trace water (i.e. 2,4-TDI produces CO₂ when reacted with water) which can be utilized to enhance the selectivity of the detection.

Detection of 2,4-TDI in Liquid and Gas Phases

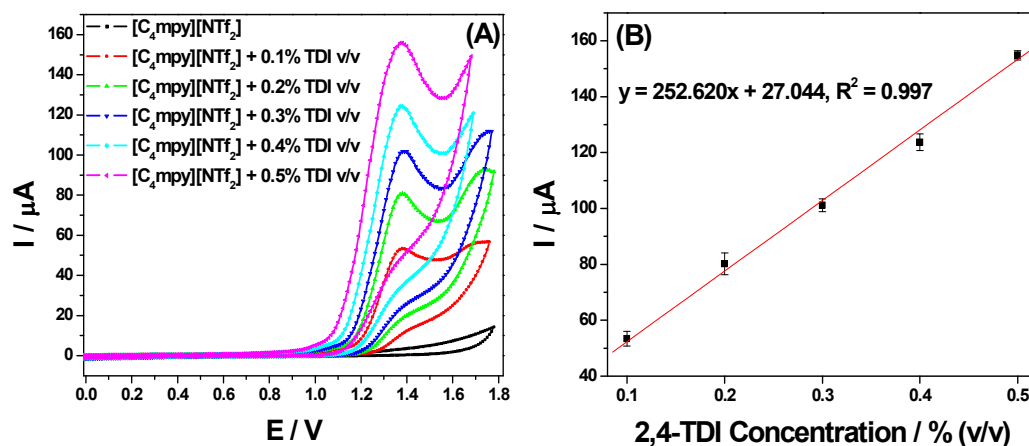


Figure 8. (A) CV sensing of liquid phase 2,4-TDI in $[\text{C}_4\text{mpy}][\text{NTf}_2]$ on glassy carbon electrode, at air conditions. Concentration of 2,4-TDI varied from 0.1% v/v to 0.5% v/v. Silver and platinum electrodes were used as the reference and counter electrodes, respectively. Scan rate was 100 mV/s. All potentials were calibrated based on Fc/Fc^+ redox couple. All curves presented here are taken from the first cycle of the CV measurements. (B) Calibration curve of the current vs. 2,4-TDI concentration, with error bars. Air is the background gas.

Finally, the sensitivity experiments are performed to evaluate LODs and T_{90} for the developed sensor mechanism. In order to perform liquid phase 2,4-TDI detection, 2,4-TDI was directly added into the electrochemical cell with $[\text{C}_4\text{mpy}][\text{NTf}_2]$ electrolyte in Air environment.

1
2
3 Concentration of 2,4-TDI were varied from 0% v/v to 0.5% v/v, with 0.1% v/v increments. The
4
5 cyclic voltammogram and the corresponding calibration curve are presented in **Figure 8**. The
6
7 value of correlation coefficient (R^2) was calculated to be 0.997. The detection sensitivity could
8
9 be obtained from the slope of the linear fitting curve, which was 252.6 $\mu\text{A}/\mu\text{L}$. By analyzing the
10
11 mean background signal (S_{bm}) and the corresponding standard deviation (s_{bm}) value, the
12
13 minimum distinguishable signal (S) can be obtained via eq. 7. Thus the limit of detection (LOD)
14
15 can then be converted from S in the calibration equation shown in **Figure 8B**. LOD in this liquid
16
17 phase 2,4-TDI sensor is 0.0651 μL in 500 μL , which equals to 130.2 ppm.

$$S = S_{\text{bm}} + 3*s_{\text{bm}} \quad (\text{eq. 7})$$

22
23
24
25
26 For gas sensing, one of the important aspect is the sampling of analyte gases. The use of
27
28 hydrophobic, non-volatile IL as an electrolyte enables a simple gas sampling system that can be
29
30 open to the ambient environment. This not only allows pre-concentration to further increase the
31
32 sensitivity of the detection but can also significantly simplify future sensor system integration
33
34 and provide long sensor lifetime. Real-time current response recording (**Figure S4**) in gas phase
35
36 sensing was performed via chronoamperometry at different 2,4-TDI concentrations. **Figure 9A**
37
38 presents the chronoamperometry data with time offset by showing the sensor response when 2,4-
39
40 TDI is added and by removing the non-faradic current decay period. Since the 2,4-TDI sample is
41
42 in liquid form, a sampling system consisting of two gas paths was designed and depicted in
43
44 **Scheme S2**. By adjusting the flowrates of the two gas paths, an accurate amount of gas phase
45
46 2,4-TDI can be calculated (i.e. the gas phase 2,4-TDI is 32.89 ppm when the flowrate of both gas
47
48 paths is 100 sccm). The external potential was set at 1.4 V, based on the cyclic voltammogram in
49
50 **Figure 8**. Each measurement was carried out in samples that were separately prepared. Air was
51
52 used as background gas in order to fully explore the real life potential of the sensor. The sensing
53
54
55
56
57
58
59
60

current reached a signal plateau at about 600th second. It is interesting to note that the sensing current curve exhibits two stages. This observation is consistent with the CV data presented in **Figure 3** and **Figure 4**, indicating that there are multiple reactions involved.

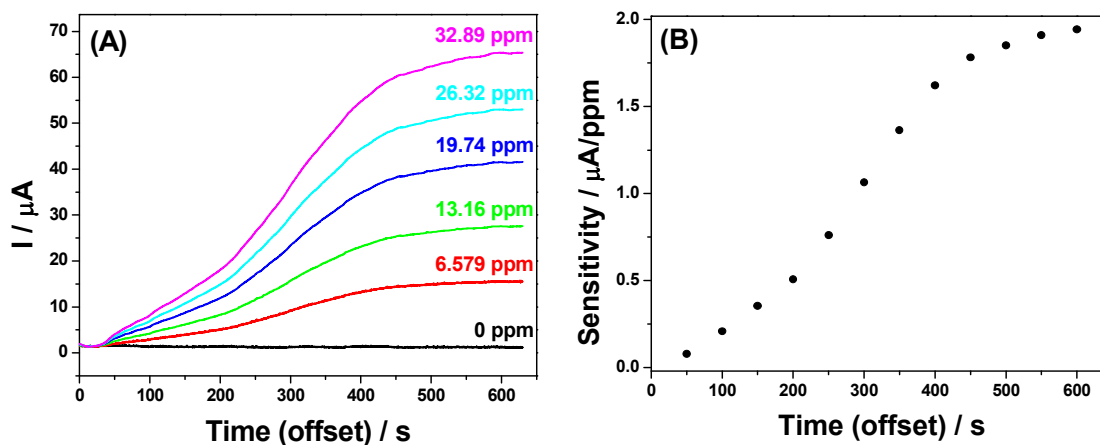


Figure 9. (A) Real time chronoamperometry detection of gas phase 2,4-TDI in $[\text{C}_4\text{mpy}][\text{NTf}_2]$. External potential was set constant at 1.4 V. Glassy carbon, silver and platinum electrodes were used as the working, reference and counter electrodes, respectively. Air was the background gas. Data sampling rate is 0.2 second per data point. (B) Plot of the selected sensitivity values at different time scales.

The plot of sensitivity values at different sensing time scales (**Figure 9B**) also demonstrates that there are two separate electrochemical steps, of which the transition point is 200th second. Detail calibration curves at various sensing time scales are shown in **Figure S5**. By analyzing the sensor response at different time scales, properties such as sensitivity and LOD values are varying (**Table S2**). For example, when picking the signal plateau at 600th second, the sensitivity is 1.942 $\mu\text{A/ppm}$ with the value of LOD to be 0.7693 ppm. But, if picking one of the time before the plateau (e.g. 100th second), the sensitivity decreases to 0.2083 $\mu\text{A/ppm}$ with a relative higher value of LOD (12.46 ppm). Besides, T90 values of this sensor to function for 100 and 600 seconds are calculated to be 90.80 seconds and 432.3 seconds, respectively. Thus, by

1
2
3 sacrificing the sensor response time, higher sensitivity and lower LOD values can be approached,
4
5 which gives this sensor a potential to tune different functioning time for different sensing needs.
6
7
8
9

10 11 12 **CONCLUSIONS** 13

14
15
16 A new electrochemical detection method was established for 2,4-TDI detection directly
17
18 in the liquid phase as well as gas phase. The sensing methodology was based on the use of non-
19
20 aqueous non-volatile IL [C₄mpy][NTf₂], which provided stable and reliable detection conditions.
21
22 Additionally, the strong ion-pairing in ILs can play a role in modifying the electrochemical
23
24 process in such a way that it can facilitate the design of sensor as in this case, the oxidation is a
25
26 single step process in ILs with lowered oxidation potential.
27
28

29
30 The detection of 2,4-TDI utilizing the oxidation process, since it has an electron-abundant
31
32 molecular structure prone to lose electrons and be oxidized, was accomplished under a set of
33
34 optimal reaction conditions which were defined as a result of detailed electrochemical study. 2,4-
35
36 TDI involved reactions were discussed in terms of reaction dynamics and the electrolyte-
37
38 electrode interface. By utilizing the IL as the electrolyte, the sensor can respond at a relatively
39
40 lower potential than other common solvents (e.g. acetonitrile). Molecules of 2,4-TDI was found
41
42 to self-accumulate and undergo inter-molecular dimerization via self-addition, suggesting a
43
44 surface modification when the TDI is measured at various time scales and the potential to
45
46 enhance selectivity. Spectroscopic methods were able to identify that the 2,4-TDI oxidation
47
48 occurred at the isocyanate functional group and the occurrence of 2,4-TDI self-addition reactions.
49
50 The selectivity experiments also provided an indirect proof of dimerization. Finally the liquid
51
52 and gas phase detection was performed with obtained detection limits capable of meeting the
53
54
55
56
57
58
59
60

1
2
3 NIOSH regulatory number (2.53 ppm). In the gas phase sensing, the sensitivity depends on the
4
5 sensing time of this sensor, with higher sensitivity at longer sensor functioning period. The use
6
7 of Clark-type electrochemical cell design³⁵ for this gas phase 2,4-TDI sensor allows the sensor to
8
9 respond in a quicker time frame, since it shortens the gas molecule diffusion process in the IL.
10
11 The uses of low cost carbon electrode material and non-volatile IL electrolyte make it a
12
13 promising low cost and miniaturized disposal sensor. The electrochemical detection based on the
14
15 oxidation of isocyanate functional group provides good selectivity and there is very little water
16
17 present in the hydrophobic IL used in this study, thus, very little isocyanates can be lost due to
18
19 the chemical reactions that occur at conventional solvents such as water, alcohol, acids and
20
21 organic solvents that contain primary and secondary amine. This benefit makes it much more
22
23 powerful and lower cost detection technology. Thus, this simple electrochemical detection could
24
25 be considered as a robust sensing method for practical detection of 2,4-TDI and might be also
26
27 applicable for the detection of other isocyanate compounds.
28
29
30
31
32
33
34
35

36 **Supplementary Information:** Schemes S1-S2, Figures S1-S5, and Table S1-S2 as noted in the
37
38 text is provided in supplementary information and is available free of charge via
39
40 <http://pubs.rsc.org>
41
42
43

44 **Author Information:** X. Zeng is the corresponding author. A. Rehman is currently working at:
45
46 Department of Chemistry, King Fahd University of Petroleum and Minerals (KFUPM), Dhahran
47
48 31261, Kingdom of Saudi Arabia (KSA)
49
50
51

52 **Acknowledgement:** X. Zeng likes to thank support of NIH R01 and Oakland University. The
53
54 authors appreciate the constructive discussion with Dr. Zhe Wang, former postdoc and currently
55
56 assistant professor at Xavier Univ. Louisiana for experiment design.
57
58
59
60

REFERENCES:

1. J. Li and B. Tian, *Science Bulletin*, 2015, **60**, 1868-1870.
2. E. B. Guglya, *J Anal Chem*, 2000, **55**, 508-529.
3. A. Pronk, E. Tielemans, G. Skarping, I. Bobeldijk, V. A. N. H. J, D. Heederik and L. Preller, *The Annals of occupational hygiene*, 2006, **50**, 1-14.
4. M.-L. Henriks-Eckerman, J. Valimaa, C. Rosenberg, K. Peltonen and K. Engstrom, *Journal of Environmental Monitoring*, 2002, **4**, 717-721.
5. U.S. Department of Health and Human Services. Hazardous Substances Data Bank (HSDB, online database). National Toxicology Information Program, National Library of Medicine, Bethesda, MD. 1993.
6. U.S. Environmental Protection Agency. EPA Chemical Profile on Toluene 2,4-Diisocyanate. 1987.
7. W. Baether, S. Zimmermann and F. Gunzer, *Sensors Journal, IEEE*, 2012, **12**, 1748-1754.
8. C. J. Tsai, H. C. Lin, T. S. Shih, K. C. Chang, I. F. Hung and C. G. Deshpande, *Journal of hazardous materials*, 2006, **137**, 1395-1401.
9. H. E. Ferreira, J. A. D. Condeco, I. O. Fernandes, D. E. Duarte and J. C. M. Bordado, *Analytical Methods*, 2014, **6**, 9242-9257.
10. G. Skarping, L. Renman, C. Sangö, L. Mathiasson and M. Dalene, *Journal of Chromatography A*, 1985, **346**, 191-204.
11. G. Skarping, M. Dalene and P. Lind, *Journal of chromatography. A*, 1994, **663**, 199-210.
12. Y. Zhu, M. Wang, H. Du, F. Wang, S. Mou and P. R. Haddad, *Journal of Chromatography A*, 2002, **956**, 215-220.
13. M. L. Chen, Y. C. Fan, C. A. Li, D. Fei and Y. Zhu, *Chinese Chemical Letters*, 2009, **20**, 207-209.
14. J. W. Schaeffer, L. M. Sargent, D. R. Sandfort and W. J. Brazile, *Journal of Occupational and Environmental Hygiene*, 2013, **10**, 213-221.
15. K. A. Kubitz, *Analytical Chemistry*, 1957, **29**, 814-816.
16. S. S. Lord, *Analytical Chemistry*, 1957, **29**, 497-499.
17. A. R. Lemons, T. A. Bledsoe, P. D. Siegel, D. H. Beezhold and B. J. Green, *Journal of Immunological Methods*, 2013, **397**, 66-70.
18. R. C. Morrison and G. G. Guilbault, *Analytical Chemistry*, 1985, **57**, 2342-2344.
19. Y. A. Tang, R. E. Edelman and S. Z. Zou, *Nanoscale*, 2014, **6**, 5630-5633.
20. H. Z. Yang, Y. G. Tang and S. Z. Zou, *Electrochemistry Communications*, 2014, **38**, 134-137.
21. L. Zhang, Q. Zhang and J. Li, *Journal of Electroanalytical Chemistry*, 2007, **603**, 243-248.
22. J. Liu, M. D. Morris, F. C. Macazo, L. R. Schoukroun-Barnes and R. J. White, *Journal of the Electrochemical Society*, 2014, **161**, H301-H313.
23. J. Liu, S. Wagan, M. D. Morris, J. Taylor and R. J. White, *Analytical Chemistry*, 2014, **86**, 11417-11424.
24. A. Rehman and X. Q. Zeng, *Accounts Chem. Res.*, 2012, **45**, 1667-1677.
25. H. T. Liu, Y. Liu and J. H. Li, *Physical Chemistry Chemical Physics*, 2010, **12**, 1685-1697.
26. X. Y. Mu, Z. Wang, X. Q. Zeng and A. J. Mason, *IEEE Sens. J.*, 2013, **13**, 3976-3981.
27. Z. G. Xia, J. H. Wang, Y. B. Hou and Q. Y. Lu, *Review of Scientific Instruments*, 2014, **85**.
28. Z. Wang, P. L. Lin, G. A. Baker, J. Stetter and X. Q. Zeng, *Analytical Chemistry*, 2011, **83**, 7066-7073.
29. Z. Wang, X. Y. Mu, M. Guo, Y. Huang, A. J. Mason and X. Q. Zeng, *J. Electrochem. Soc.*, 2013, **160**, B83-B89.
30. C. H. Xiao, A. Rehman and X. Q. Zeng, *Analytical Chemistry*, 2012, **84**, 1416-1424.

- 1
 - 2
 - 3
 - 4
 - 5
 - 6
 - 7
 - 8
 - 9
 - 10
 - 11
 - 12
 - 13
 - 14
 - 15
 - 16
 - 17
 - 18
 - 19
 - 20
 - 21
 - 22
 - 23
 - 24
 - 25
 - 26
 - 27
 - 28
 - 29
 - 30
 - 31
 - 32
 - 33
 - 34
 - 35
 - 36
 - 37
 - 38
 - 39
 - 40
 - 41
 - 42
 - 43
 - 44
 - 45
 - 46
 - 47
 - 48
 - 49
 - 50
 - 51
 - 52
 - 53
 - 54
 - 55
 - 56
 - 57
 - 58
 - 59
 - 60
31. C. Xiao, A. Rehman and X. Zeng, *RSC Advances*, 2015, **5**, 31826-31836.
32. Z. Wang and X. Q. Zeng, *J. Electrochem. Soc.*, 2013, **160**, H604-H611.
33. C. H. Xiao and X. Q. Zeng, *Journal of the Electrochemical Society*, 2013, **160**, H749-H756.
34. Relative reactivity of isocyanates with active hydrogen compounds.
<http://www.poliuretanos.com.br/Ingles/Chapter1/131Isocyanates.htm>
35. New Jersey Department of Health and Senior Services "Hazardous Substance Fact Sheet"
36. A. Rehman, A. Hamilton, A. Chung, G. A. Baker, Z. Wang and X. Q. Zeng, *Analytical Chemistry*, 2011, **83**, 7823-7833.
37. A. Atifi and M. D. Ryan, *Analytical Chemistry*, 2014, **86**, 6617-6625.
38. A. J. Fry, *Electrochemistry Communications*, 2005, **7**, 602-606.
39. Z. Wang, M. Guo, G. A. Baker, J. R. Stetter, L. Lin, A. J. Mason and X. Q. Zeng, *Analyst*, 2014, **139**, 5140-5147.
40. D. T. Sawyer and J. S. Valentine, *Accounts of Chemical Research*, 1981, **14**, 393-400.
41. Y. Kuroiwa, Y. Kato and T. Watanabe, *Journal of Photochemistry and Photobiology A: Chemistry*, 2009, **202**, 191-195.
42. H. P. de Oliveira and C. P. de Melo, *Journal of Physical Chemistry B*, 2011, **115**, 6903-6908.
43. <https://www2.chemistry.msu.edu/faculty/reusch/VirtTxtJml/Spectrpy/UV-Vis/spectrum.htm>
44. M. A. Thomson, P. J. Melling and A. M. Slepiski, *Abstracts of Papers of the American Chemical Society*, 2001, **221**, U316-U316.
45. Y. Yakabe, K. M. Henderson, W. C. Thompson, D. Pemberton, B. Tury and R. E. Bailey, *Environmental Science & Technology*, 1999, **33**, 2579-2583.